Earthquakes and Structures, *Vol. 11, No. 1 (2016) 63-82*
DOI: http://dx.doi.org/10.12989/eas.2016.11.1.063

An efficient and simple higher order shear deformation theory for bending analysis of composite plates under various boundary conditions

Belkacem Adim[1,2], Tahar Hassaine Daouadji[*1,2], Benferhat Rabia[3] and Lazreg Hadji[1,2]

[1]*Département de Génie Civil, Université Ibn Khaldoun Tiaret; BP 78 Zaaroura, 14000 Tiaret, Algérie*
[2]*Laboratoire de Géomatique et Développement Durable, Université Ibn Khaldoun de Tiaret Algérie*
[3]*Laboratoire de Géomatériaux , Département de Génie Civil, Université de Chlef, Algérie*

(Received November 8, 2015, Revised May 27, 2016, Accepted June 15, 2016)

Abstract. In this study, the bending and dynamic behaviors of laminated composite plates is examined by using a refined shear deformation theory and developed for a bending analysis of orthotropic laminated composite plates under various boundary conditions. The displacement field of the present theory is chosen based on nonlinear variations in the in-plane displacements through the thickness of the plate. By dividing the transverse displacement into the bending and shear parts and making further assumptions, the number of unknowns and equations of motion of the present theory is reduced and hence makes them simple to use. In the analysis, the equation of motion for simply supported thick laminated rectangular plates is obtained through the use of Hamilton's principle. Numerical results for the bending and dynamic behaviors of antisymmetric cross-ply laminated plate under various boundary conditions are presented. The validity of the present solution is demonstrated by comparison with solutions available in the literature. Numerical results show that the present theory can archive accuracy comparable to the existing higher order shear deformation theories that contain more number of unknowns.

Keywords: higher-order theories; shear deformation theory of plates; laminated composite plate

1. Introduction

The use of composite material for the structure/component design has grown significantly over the last few decades because their response characteristics can be tailored to meet specific design requirements. Furthermore, composite structures possess high specific stiffness and high specific strength which leads to overall reduction of weight, by increasing the efficiency of the structure. Currently, laminate composite are widely used in many structural applications. Due to the high degrees of anisotropy and the low rigidity in transverse shear of the plates, the Kirchhoff hypothesis as a classical theory is no longer adequate. The hypothesis states that the normal to the midplane of a plate remains straight and normal after deformation because of the negligible

*Corresponding author, Professor, E-mail: daouadjitahar@gmail.com

http://www.techno-press.com/journals/eas&subpage=7 ISSN: 2092-7614 (Print), 2092-7622 (Online)

transverse shear effects. However, the classical theory under predicts deflections and over predicts frequencies as well as buckling loads with moderately thick plates. Many shear deformation theories account for transverse shear effects have been developed to overcome the deficiencies of the CLPT. The first-order shear deformation theories based on Reissner (1945) and Mindlin (1951) account for the transverse shear effects by the way of linear variation of in-plane displacements through the thickness. Since first-order violates equilibrium conditions at the top and bottom faces of the plate, shear correction factors are required to rectify the unrealistic variation of the shear strain/stress through the thickness. In order to overcome the limitations of that theory (first-order), higher-order shear deformation theories, which involve higher-order terms in Taylor's expansions of the displacements in the thickness coordinate, were developed by Reddy (1984), Zenkour (2006), Tounsi *et al*. (2013), Hassaine Daouadji *et al*. (2013), Benferhat *et al*. (2014), Nedri *et al.* (2014), Abdelhak *et al*. (2014), Mahi *et al*. (2015) Mantari (2012) and Ren (2014), and Hebali *et al*. (2014). A good review of these theories for the analysis of laminated composite plates is available in the work of Karama (2009), Reddy (1986), Aydogdu (2009), Meiche (2011). A two variable refined plate theory using only two unknown functions was developed by Shimpi (2002), Bouazza *et al*. (2015) and Tlidji (2014) for isotropic plates, and was extended by Shimpi and Patel (2006) for orthotropic plates. The most interesting feature of this theory is that it does not require shear correction factor, and has strong similarities with the classical plate theory in some aspects such as governing equation, boundary conditions and moment expressions.

In this paper, a simple higher order shear order deformation theory of plates is developed and applied to the investigation of static and dynamic behavior of laminated composite plates. The present theory is based on the assumption that the in-plane and transverse displacements consist of bending and shear components where the bending components do not contribute to shear forces, and likewise, the shear components do not contribute to bending moments. The most interesting feature of this theory is that it allows for parabolic distributions of transverse shear stresses across the plate thickness and satisfies zero shear stress conditions at the top and bottom surfaces of the plate without using shear correction factors. The equations of motion are derived using Hamilton's principle. The fundamental frequencies are found by solving an Eigen value equation. The results obtained by the present method are compared with solutions and results of the first-order and the other higher-order theories.

2. Theoretical formulations

2.1 Basic assumptions

Consider a rectangular plate of total thickness $\boldsymbol{h}$ composed of n orthotropic layers with the coordinate system as shown in Fig. 1. Assumptions of the refined plate's theory are as follows:

- The displacements are small in comparison with the plate thickness and, therefore, strains involved are infinitesimal.

- The transverse displacement $\boldsymbol{w}$ includes three components of bending $\boldsymbol{w_b}$ and shear $\boldsymbol{w_s}$. These components are functions of coordinates x, y, and time t only

$$w(x,y,z,t) = w_b(x,y,t) + w_s(x,y,t) \tag{1}$$

- The transverse normal stress σ_z is negligible in comparison with in-plane stresses σ_x and σ_y.

- The displacements U in x-direction and V in y-direction consist of extension, bending, and shear

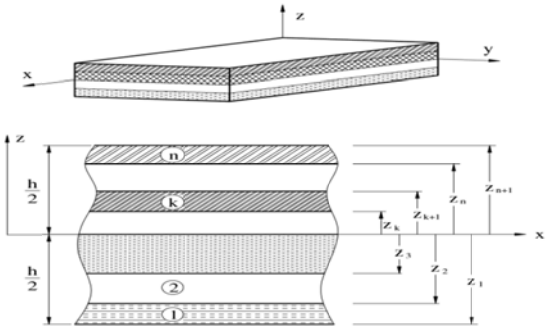

Fig. 1 Coordinate system and layer numbering used for a typical laminated plate

components

$$U = u + u_b + u_s, \qquad V = v + v_b + v_s \tag{2}$$

The bending components u_b and v_b are assumed to be similar to the displacements given by the classical plate theory. Therefore, the expression for u_b and v_b can be given as

$$u_b = -z\frac{\partial w_b}{\partial x}, \qquad v_b = -z\frac{\partial w_b}{\partial y} \tag{3}$$

The shear components u_s and v_s give rise, in conjunction with w_s, to the parabolic variations of shear strains γ_{xz}, γ_{yz} and hence to shear stresses σ_{xz}, σ_{yz} through the thickness of the plate in such a way that shear stresses σ_{xz}, σ_{yz} are zero at the top and bottom faces of the plate. Consequently, the expression for u_s and v_s can be given as

$$u_s = f(z)\frac{\partial w_s}{\partial x}, \qquad v_s = f(z)\frac{\partial w_s}{\partial y} \tag{4}$$

2.2 Kinematics

Based on the assumptions made in the preceding section, the displacement field can be obtained using Eqs. (1)-(4)

$$\begin{aligned} u(x,y,z,t) &= u_0(x,y,t) - z\frac{\partial w_b}{\partial x} - f(z)\frac{\partial w_s}{\partial x} \\ v(x,y,z,t) &= v_0(x,y,t) - z\frac{\partial w_b}{\partial y} - f(z)\frac{\partial w_s}{\partial y} \\ w(x,y,z,t) &= w_b(x,y,t) + w_s(x,y,t) \end{aligned} \tag{5a}$$

where u_0 and v_0 are the mid-plane displacements of the plate in the x and y direction, respectively; w_b and w_s are the bending and shear components of transverse displacement, respectively, while $f(z)$ represents shape functions determining the distribution of the transverse shear strains and stresses along the thickness, This function ensures zero transverse shear stresses at the top and bottom surfaces of the plate. The parabolic distributions of transverse shear stresses across the plate thickness are taken into account in the analysis by means of present function the assumed displacement field, and is given as:

Present model SSDT: The function *f*(z) is an sinusoidal shape function (Sinusoidal Shear Deformation Theory) (Benferhat *et al*. 2014)

$$f(z) = z - \sin\left(\frac{\pi z}{h}\right) \tag{5b}$$

The strains associated with the displacements in Eq. (5) are

$$\begin{Bmatrix} \varepsilon_x \\ \varepsilon_y \\ \gamma_{xy} \end{Bmatrix} = \begin{Bmatrix} \varepsilon_x^0 \\ \varepsilon_y^0 \\ \gamma_{xy}^0 \end{Bmatrix} + z \begin{Bmatrix} k_x^b \\ k_y^b \\ k_{xy}^b \end{Bmatrix} + f(z) \begin{Bmatrix} k_x^s \\ k_y^s \\ k_{xy}^s \end{Bmatrix}, \qquad \begin{Bmatrix} \gamma_{yz} \\ \gamma_{xz} \end{Bmatrix} = g(z) \begin{Bmatrix} \gamma_{yz}^s \\ \gamma_{xz}^s \end{Bmatrix} \tag{6a}$$

where

$$\begin{Bmatrix} \varepsilon_x^0 \\ \varepsilon_y^0 \\ \gamma_{xy}^0 \end{Bmatrix} = \begin{Bmatrix} \dfrac{\partial u_0}{\partial x} \\ \dfrac{\partial v_0}{\partial y} \\ \dfrac{\partial u_0}{\partial y} + \dfrac{\partial v_0}{\partial x} \end{Bmatrix}, \quad \begin{Bmatrix} k_x^b \\ k_y^b \\ k_{xy}^b \end{Bmatrix} = \begin{Bmatrix} -\dfrac{\partial^2 w_b}{\partial x^2} \\ -\dfrac{\partial^2 w_b}{\partial y^2} \\ -2\dfrac{\partial^2 w_b}{\partial x \partial y} \end{Bmatrix}, \quad \begin{Bmatrix} k_x^s \\ k_y^s \\ k_{xy}^s \end{Bmatrix} = \begin{Bmatrix} -\dfrac{\partial^2 w_s}{\partial x^2} \\ -\dfrac{\partial^2 w_s}{\partial y^2} \\ -2\dfrac{\partial^2 w_s}{\partial x \partial y} \end{Bmatrix}, \quad \begin{Bmatrix} \gamma_{yz}^s \\ \gamma_{xz}^s \end{Bmatrix} = \begin{Bmatrix} \dfrac{\partial w_s}{\partial y} \\ \dfrac{\partial w_s}{\partial x} \end{Bmatrix} \tag{6b}$$

And: $g(z) = 1 - f'(z)$, $f'(z) = \dfrac{df(z)}{dz}$

2.3 Constitutive equations

The stress state in each layer is given by Hooke's law

$$\begin{Bmatrix} \sigma_x \\ \sigma_y \\ \tau_{xy} \\ \tau_{yz} \\ \tau_{xz} \end{Bmatrix} = \begin{bmatrix} Q_{11} & Q_{12} & 0 & 0 & 0 \\ Q_{12} & Q_{22} & 0 & 0 & 0 \\ 0 & 0 & Q_{66} & 0 & 0 \\ 0 & 0 & 0 & Q_{44} & 0 \\ 0 & 0 & 0 & 0 & Q_{55} \end{bmatrix} \begin{Bmatrix} \varepsilon_x \\ \varepsilon_y \\ \gamma_{xy} \\ \gamma_{yz} \\ \gamma_{xz} \end{Bmatrix} \tag{7a}$$

Where Q_{ij} are the stiffness's, which are defined in terms of engineering constants in the material axes of the layer

$$Q_{11} = \frac{E_{11}}{1 - \nu_{12}\nu_{21}}, \quad Q_{22} = \frac{E_{22}}{1 - \nu_{12}\nu_{21}}, \quad Q_{12} = \frac{\nu_{12}E_{22}}{1 - \nu_{12}\nu_{21}}, \quad Q_{66} = G_{12}, \quad Q_{44} = G_{23}, \quad Q_{55} = G_{13} \tag{7b}$$

Since the laminate is made of several orthotropic layers with their material axes oriented arbitrarily with respect to laminate coordinates, the constitutive equations of each layer must be transformed to the laminate coordinates *x*, *y*, and z. The stress-strain relations in the laminate coordinates of a kth layer are

$$\begin{Bmatrix} \sigma_x \\ \sigma_y \\ \tau_{xy} \\ \tau_{yz} \\ \tau_{xz} \end{Bmatrix}^{(k)} = \begin{bmatrix} \overline{Q}_{11} & \overline{Q}_{12} & \overline{Q}_{16} & 0 & 0 \\ \overline{Q}_{12} & \overline{Q}_{22} & \overline{Q}_{26} & 0 & 0 \\ \overline{Q}_{16} & \overline{Q}_{26} & \overline{Q}_{66} & 0 & 0 \\ 0 & 0 & 0 & \overline{Q}_{44} & \overline{Q}_{45} \\ 0 & 0 & 0 & \overline{Q}_{45} & \overline{Q}_{55} \end{bmatrix}^{(k)} \begin{Bmatrix} \varepsilon_x \\ \varepsilon_y \\ \gamma_{xy} \\ \gamma_{yz} \\ \gamma_{xz} \end{Bmatrix}^{(k)} \tag{7c}$$

Where $\overline{Q}_{ij}$ are the transformed material constants, which a given in (Karama 2003) as

$$\begin{aligned} \overline{Q}_{11} &= Q_{11}\cos^4\theta + 2(Q_{12} + 2Q_{66})\sin^2\theta\cos^2\theta + Q_{22}\sin^4\theta \\ \overline{Q}_{12} &= (Q_{11} + Q_{22} - 4Q_{66})\sin^2\theta\cos^2\theta + Q_{12}(\sin^4\theta + \cos^4\theta) \\ \overline{Q}_{22} &= Q_{11}\sin^4\theta + 2(Q_{12} + 2Q_{66})\sin^2\theta\cos^2\theta + Q_{22}\cos^4\theta \\ \overline{Q}_{16} &= (Q_{11} - Q_{12} - 2Q_{66})\sin\theta\cos^3\theta + (Q_{12} - Q_{22} + 2Q_{66})\sin^3\theta\cos\theta \\ \overline{Q}_{26} &= (Q_{11} - Q_{12} - 2Q_{66})\sin^3\theta\cos\theta + (Q_{12} - Q_{22} + 2Q_{66})\sin\theta\cos^3\theta \\ \overline{Q}_{66} &= (Q_{11} + Q_{22} - 2Q_{12} - 2Q_{66})\sin^2\theta\cos^2\theta + Q_{66}(\sin^4\theta + \cos^4\theta) \\ \overline{Q}_{44} &= Q_{44}\cos^2\theta + Q_{55}\sin^2\theta \\ \overline{Q}_{45} &= (Q_{55} - Q_{44})\cos\theta\sin\theta \\ \overline{Q}_{55} &= Q_{55}\cos^2\theta + Q_{44}\sin^2\theta \end{aligned} \tag{7d}$$

In which θ is the angle between the global x-axis and the local x-axis of each layer.

2.4 Governing equations

Using Hamilton's energy principle, we derive the equation of motion of the laminated composite plate

$$\delta\int_{t_1}^{t_2}(U - V - T)dt = 0 \tag{8a}$$

Where *U* is the strain energy, *T* is the kinetic energy of the plate, and *V* is the work of external forces. Employing the principle of minimum total energy leads to the general equation of motion and boundary conditions. Taking the variation of the above equation and integrating by parts, we obtain

$$\begin{aligned} \int_{t_2}^{t_1} \Bigg[\int_V & (\sigma_x\delta\varepsilon_x + \sigma_y\delta\varepsilon_y + \tau_{xy}\delta\gamma_{xy} + \tau_{yz}\delta\gamma_{yz} + \tau_{xz}\delta\gamma_{xz}) \\ & - \rho(\ddot{u}_0\delta u_0 + \ddot{v}_0\delta v_0 + (\ddot{w}_b + \ddot{w}_s)\delta(w_b + w_s))\,dV - \int_A q\,\delta(w_b + w_s)\,dA \Bigg] dt = 0 \end{aligned} \tag{8b}$$

Where q is the transverse load, and two points above a variable means the second derivative with respect to time. With account of Eqs. (6), Eq. (8) takes the form

$$\begin{aligned}
&\int_{t_2}^{t_1}\Bigg[\int_A \Big(-\delta u_0 N_{x,x} - \delta v_0 N_{y,y} - \delta u_0 N_{xy,y} - \delta v_0 N_{xy,x} - \delta w_b M^b_{x,xx} - \delta w_b M^b_{y,yy} - 2\delta w_b M^b_{xy,xy} \\
&- \delta w_s M^s_{x,xx} - \delta w_s M^s_{y,yy} - 2\delta w_s M^s_{xy,xy} - \delta w_s S^s_{xz,x} - \delta w_s S^s_{yz,y}\Big) dA - \int_A q\,\delta(w_b + w_s)\,dA \\
&- \int_A \Big\{\delta u_0 \left(I_1 \ddot{u}_0 - I_2 \ddot{w}_{b,x} - I_4 \ddot{w}_{s,x}\right) + \delta v_0 \left(I_1 \ddot{v}_0 - I_2 \ddot{w}_{b,y} - I_4 \ddot{w}_{s,y}\right) \\
&+ \delta w_b \left[I_1(\ddot{w}_b + \ddot{w}_s) + I_2(\ddot{u}_{0,x} + \ddot{v}_{o,y}) - I_3(\ddot{w}_{b,xx} + \ddot{w}_{b,yy}) - I_5(\ddot{w}_{s,xx} + \ddot{w}_{s,yy})\right] \\
&+ \delta w_s \left[I_1(\ddot{w}_b + \ddot{w}_s) + I_4(\ddot{u}_{0,x} + \ddot{v}_{o,y}) - I_5(\ddot{w}_{b,xx} + \ddot{w}_{b,yy}) - I_6(\ddot{w}_{s,xx} + \ddot{w}_{s,yy})\right]\Big\} dA \Bigg] dt = 0
\end{aligned} \tag{9}$$

The stress resultants N, M and S are defined as

$$(N_x, N_y, N_{xy}) = \int_{-h/2}^{h/2} (\sigma_x, \sigma_y, \tau_{xy})\, dz = \sum_{k=1}^{N} \int_{z_k}^{z_{k+1}} (\sigma_x, \sigma_y, \tau_{xy})\, dz \tag{10a}$$

$$(M^b_x, M^b_y, M^b_{xy}) = \int_{-h/2}^{h/2} (\sigma_x, \sigma_y, \tau_{xy})\, z\, dz = \sum_{k=1}^{N} \int_{z_k}^{z_{k+1}} (\sigma_x, \sigma_y, \tau_{xy})\, z\, dz \tag{10b}$$

$$(M^s_x, M^s_y, M^s_{xy}) = \int_{-h/2}^{h/2} (\sigma_x, \sigma_y, \tau_{xy})\, f(z)\, dz = \sum_{k=1}^{N} \int_{z_k}^{z_{k+1}} (\sigma_x, \sigma_y, \tau_{xy})\, f(z)\, dz \tag{10c}$$

$$(S^s_{xz}, S^s_{yz}) = \int_{-h/2}^{h/2} (\tau_{xz}, \tau_{yz})\, g(z)\, dz = \sum_{k=1}^{N} \int_{z_k}^{z_{k+1}} (\tau_{xz}, \tau_{yz})\, g(z)\, dz \tag{10d}$$

Inserting Eq. (7) into Eqs. (10) and integrating across the thickness of the plate, the stress resultants are obtained

$$\begin{Bmatrix} N \\ M^b \\ M^s \end{Bmatrix} = \begin{bmatrix} A & B & B^s \\ B & D & D^s \\ B^s & D^s & H^s \end{bmatrix} \begin{Bmatrix} \varepsilon \\ k^b \\ k^s \end{Bmatrix}, , \quad \begin{Bmatrix} S^s_{yz} \\ S^s_{xz} \end{Bmatrix} = \begin{bmatrix} A^s_{44} & A^s_{45} \\ A^s_{45} & A^s_{55} \end{bmatrix} \begin{Bmatrix} \gamma^s_{yz} \\ \gamma^s_{xz} \end{Bmatrix} \tag{11a}$$

Where

$$N = \{N_x, N_y, N_{xy}\}^t, \quad M^b = \{M^b_x, M^b_y, M^b_{xy}\}^t, \quad M^s = \{M^s_x, M^s_y, M^s_{xy}\}^t, \tag{11b}$$

$$\varepsilon = \{\varepsilon^0_x, \varepsilon^0_y, \gamma^0_{xy}\}, \qquad k^b = \{k^b_x, k^b_y, k^b_{xy}\}, \qquad k^s = \{k^s_x, k^s_y, k^s_{xy}\} \tag{11c}$$

$$A = \begin{bmatrix} A_{11} & A_{12} & A_{16} \\ A_{12} & A_{22} & A_{26} \\ A_{16} & A_{26} & A_{66} \end{bmatrix}, \quad B = \begin{bmatrix} B_{11} & B_{12} & B_{16} \\ B_{12} & B_{22} & B_{26} \\ B_{16} & B_{26} & B_{66} \end{bmatrix}, \quad D = \begin{bmatrix} D_{11} & D_{12} & D_{16} \\ D_{12} & D_{22} & D_{26} \\ D_{16} & D_{26} & D_{66} \end{bmatrix} \tag{11d}$$

$$B^s = \begin{bmatrix} B^s_{11} & B^s_{12} & B^s_{16} \\ B^s_{12} & B^s_{22} & B^s_{26} \\ B^s_{16} & B^s_{26} & B^s_{66} \end{bmatrix}, \quad D^s = \begin{bmatrix} D^s_{11} & D^s_{12} & D^s_{16} \\ D^s_{12} & D^s_{22} & D^s_{26} \\ D^s_{16} & D^s_{26} & D^s_{66} \end{bmatrix}, \quad H^s = \begin{bmatrix} H^s_{11} & H^s_{12} & H^s_{16} \\ H^s_{12} & H^s_{22} & H^s_{26} \\ H^s_{16} & H^s_{26} & H^s_{66} \end{bmatrix} \tag{11e}$$

And the stiffness components and inertias are given as

$$\left(A_{ij}, B_{ij}, D_{ij}, B_{ij}^{s}, D_{ij}^{s}, H_{ij}^{s}\right)=\int_{-h/2}^{h/2} \overline{Q_{ij}}\,(1, z, z^{2}, f(z), zf(z), f^{2}(z))\,dz \quad , \quad (i, j)=(1,2,6) \tag{12a}$$

$$A_{ij}^{s}=\int_{-h/2}^{h/2} \overline{Q_{ij}}\,[g(z)]^{2}\,dz \quad ,(i, j)=(4,5) \tag{12b}$$

$$(I_{1}, I_{2}, I_{3}, I_{4}, I_{5}, I_{6})=\int_{-h/2}^{h/2} \rho\,(1, z, z^{2}, f(z), zf(z), [f(z)]^{2})\,dz \tag{12c}$$

Collecting the coefficients of δ_{u0}, δ_{v0}, δ_{wb} and δ_{ws} in Eq. (9), the equations of motion are obtained as

$$\begin{aligned}
\delta u_{0}&: N_{x,x}+N_{xy,y}=I_{1}\ddot{u}_{0}-I_{2}\ddot{w}_{b,x}-I_{4}\ddot{w}_{s,x}\\
\delta v_{0}&: N_{xy,x}+N_{y,y}=I_{1}\ddot{v}_{0}-I_{2}\ddot{w}_{b,y}-I_{4}\ddot{w}_{s,y}\\
\delta w_{b}&: M_{x,xx}^{b}+2M_{xy,xy}^{b}+M_{y,yy}^{b}+q=I_{1}(\ddot{w}_{b}+\ddot{w}_{s})+I_{2}(\ddot{u}_{0,x}+\ddot{v}_{0,y})\\
&\qquad -I_{3}(\ddot{w}_{b,xx}+\ddot{w}_{b,yy})-I_{5}(\ddot{w}_{s,xx}+\ddot{w}_{s,yy})\\
\delta w_{s}&: M_{x,xx}^{s}+2M_{xy,xy}^{s}+M_{y,yy}^{s}+S_{xz,x}^{s}+S_{yz,y}^{s}+q=I_{1}(\ddot{w}_{b}+\ddot{w}_{s})+I_{4}(\ddot{u}_{0,x}+\ddot{v}_{0,y})\\
&\qquad -I_{5}(\ddot{w}_{b,xx}+\ddot{w}_{b,yy})-I_{6}(\ddot{w}_{s,xx}+\ddot{w}_{s,yy})
\end{aligned} \tag{13}$$

Clearly, when the effect of transverse shear deformation is neglected (w_s =0), Eqs. (13) yield the equations of motion of a composite plate based on the classical theory of plates.

3. Analytical solution for antisymmetric cross-ply laminates

For antisymmetric cross-ply laminates, the following plate stiffnesses are identically zero

$$\begin{gathered}
A_{16}=A_{26}=D_{16}=D_{26}=D_{16}^{s}=D_{26}^{s}=H_{16}^{s}=H_{26}^{s}=0\;,\; B_{22}=-B_{11}\;,\\
B_{22}^{s}=-B_{11}^{s}\\
B_{12}=B_{26}=B_{16}=B_{66}=B_{12}^{s}=B_{16}^{s}=B_{26}^{s}=B_{66}^{s}=A_{45}^{s}=0
\end{gathered} \tag{14}$$

The exact solution of Eqs. (13) for the antisymmetric cross-ply laminated plate under various boundary conditions can be constructed according to (Ait Amar *et al.* 2014). The boundary conditions for an arbitrary edge with simply supported and clamped edge conditionare:

• Clamped (C)

$$u=v=w_{b}=w_{s}=\frac{\partial w_{b}}{\partial x}=\frac{\partial w_{b}}{\partial y}=\frac{\partial w_{s}}{\partial x}=\frac{\partial w_{s}}{\partial y}=0 \quad \text{at} \quad x=0, a \quad \text{and} \quad y=0, b \tag{15}$$

• Simply supported (S)

$$v=w_{b}=w_{s}=\frac{\partial w_{b}}{\partial y}=\frac{\partial w_{s}}{\partial y}=0 \quad \text{at} \quad x=0, a \tag{16a}$$

$$u=w_{b}=w_{s}=\frac{\partial w_{b}}{\partial x}=\frac{\partial w_{s}}{\partial x}=0 \quad \text{at} \quad y=0, b \tag{16b}$$

The boundary conditions in Eqs. (15) and (16) are satisfied by the following expansions

$$
\begin{aligned}
u &= U_{mn} X'_m(x)\, Y_n(y) e^{(i\omega t)} \\
v &= V_{mn}\, X_m(x)\, Y'_n(y) e^{(i\omega t)} \\
w_b &= W_{bmn}\;\; X_m(x)\, Y_n(y) e^{(i\omega t)} \\
w_s &= W_{smn}\;\; X_m(x)\, Y_n(y) e^{(i\omega t)}
\end{aligned}
\tag{17}
$$

Where U_{mn}, V_{mn}, W_{bmn} *and* W_{smn} unknown parameters must be determined, ω is the Eigen frequency associated with (m, n) the Eigen-mode. The functions $X_m(x)$ and $Y_n(y)$ are suggested here to satisfy at least the geometric boundary conditions given in Eqs. (15) and (16) and represent approximate shapes of the deflected surface of the plate. These functions, for the different cases of boundary conditions, are listed in Table 1, with $\lambda = \dfrac{m\pi}{a}$ and $\mu = \dfrac{n\pi}{b}$.

Substituting Eqs. (17) and (14) into Eq. (13), the exact solution of antisymmetric cross-ply laminates can be determined from equations

$$
\left(\begin{bmatrix} a_{11} & a_{12} & a_{13} & a_{14} \\ a_{12} & a_{22} & a_{23} & a_{24} \\ a_{13} & a_{23} & a_{33} & a_{34} \\ a_{14} & a_{24} & a_{34} & a_{44} \end{bmatrix} - \omega^2 \begin{bmatrix} m_{11} & 0 & m_{13} & m_{14} \\ 0 & m_{22} & m_{23} & m_{24} \\ m_{31} & m_{32} & m_{33} & m_{34} \\ m_{41} & m_{42} & m_{34} & ms_{44} \end{bmatrix} \right) \begin{Bmatrix} U_{mn} \\ V_{mn} \\ W_{bmn} \\ W_{smn} \end{Bmatrix} = \begin{Bmatrix} 0 \\ 0 \\ q \\ q \end{Bmatrix}
\tag{18}
$$

Where

$$
\begin{aligned}
a_{11} &= \int_0^a \int_0^b \left(A_{11} X'''_m Y_n + A_{66} X'_m Y''_n \right) X'_m Y_n \, dxdy \\
a_{12} &= \int_0^a \int_0^b \left(A_{12} + A_{66} \right) X'_m Y''_n X'_m Y_n \, dxdy \\
a_{13} &= -\int_0^a \int_0^b \left[B_{11} X''_m Y_n + \left(B_{12} + 2B_{66} \right) X'_m Y''_n \right] X'_m Y_n \, dxdy \\
a_{14} &= -\int_0^a \int_0^b \left[B^s_{11} X''_m Y_n + \left(B^s_{12} + 2B^s_{66} \right) X'_m Y''_n \right] X'_m Y_n \, dxdy \\
a_{21} &= \int_0^a \int_0^b \left(A_{12} + A_{66} \right) X''_m Y'_n X_m Y'_n \, dxdy \\
a_{22} &= \int_0^a \int_0^b \left(A_{22} X_m Y'''_n + A_{66} X''_m Y'_n \right) X_m Y'_n \, dxdy \\
a_{23} &= -\int_0^a \int_0^b \left[B_{22} X_m Y'''_n + \left(B_{12} + 2B_{66} \right) X''_m Y'_n \right] X_m Y'_n \, dxdy \\
a_{24} &= -\int_0^a \int_0^b \left[B^s_{22} X_m Y'''_n + \left(B^s_{12} + 2B^s_{66} \right) X''_m Y'_n \right] X_m Y'_n \, dxdy \\
a_{31} &= \int_0^a \int_0^b \left[B_{11} X''''_m Y_n + \left(B_{12} + 2B_{66} \right) X''_m Y''_n \right] X_m Y_n \, dxdy \\
a_{32} &= \int_0^a \int_0^b \left[B_{22} X_m Y''''_n + \left(B_{12} + 2B_{66} \right) X''_m Y''_n \right] X_m Y_n \, dxdy
\end{aligned}
\tag{19}
$$

$$
a_{33} = \int_0^a \int_0^b - \left[D_{11} X''''_m Y_n + 2\left(D_{12} + 2D_{66} \right) X''_m Y''_n + D_{22} X_m Y''''_n \right] X_m Y_n \, dxdy
\tag{19}
$$

$$a_{34} = \int_0^a \int_0^b -\left[D_{11}^s X_m'''' Y_n + 2\left(D_{12}^s + 2D_{66}^s\right) X_m'' Y_n'' + D_{22}^s X_m Y_n''''\right] X_m Y_n \, dxdy$$

$$a_{41} = \int_0^a \int_0^b \left[B_{11}^s X_m'''' Y_n + \left(B_{12}^s + 2B_{66}^s\right) X_m'' Y_n''\right] X_m Y_n \, dxdy$$

$$a_{42} = \int_0^a \int_0^b \left[B_{22}^s X_m Y_n'''' + \left(B_{12}^s + 2B_{66}^s\right) X_m'' Y_n''\right] X_m Y_n \, dxdy$$

$$a_{43} = \int_0^a \int_0^b -\left[D_{11}^s X_m'''' Y_n + 2\left(D_{12}^s + 2D_{66}^s\right) X_m'' Y_n'' + D_{22}^s X_m Y_n''''\right] X_m Y_n \, dxdy$$

$$a_{44} = \int_0^a \int_0^b -\left[H_{11}^s X_m'''' Y_n + 2\left(H_{12}^s + 2H_{66}^s\right) X_m'' Y_n'' + H_{22}^s X_m Y_n'''' - A_{55}^s X_m'' Y_n - A_{44}^s X_m Y_n''\right] X_m Y_n \, dxdy$$

$$m_{11} = \int_0^a \int_0^b - I_1 X_m' Y_n X_m' Y_n \, dxdy$$

$$m_{13} = \int_0^a \int_0^b I_2 X_m' Y_n X_m' Y_n \, dxdy$$

$$m_{14} = \int_0^a \int_0^b I_4 X_m' Y_n X_m' Y_n \, dxdy$$

$$m_{22} = \int_0^a \int_0^b - I_1 X_m Y_n' X_m Y_n' \, dxdy$$

$$m_{23} = \int_0^a \int_0^b I_2 X_m Y_n' X_m Y_n' \, dxdy$$

$$m_{24} = \int_0^a \int_0^b I_4 X_m Y_n' X_m Y_n' \, dxdy$$

$$m_{31} = \int_0^a \int_0^b - I_2 X_m Y_n X_m'' Y_n \, dxdy$$

$$m_{32} = \int_0^a \int_0^b - I_2 X_m Y_n X_m Y_n'' \, dxdy$$

$$m_{33} = \int_0^a \int_0^b - I_1 X_m Y_n X_m Y_n \, dxdy + \int_0^a \int_0^b I_3 X_m Y_n X_m Y_n'' \, dxdy + \int_0^a \int_0^b I_3 X_m Y_n X_m'' Y_n \, dxdy$$

$$m_{34} = \int_0^a \int_0^b - I_1 X_m Y_n X_m Y_n \, dxdy + \int_0^a \int_0^b I_5 X_m Y_n X_m Y_n'' \, dxdy + \int_0^a \int_0^b I_5 X_m Y_n X_m'' Y_n \, dxdy$$

$$m_{41} = \int_0^a \int_0^b - I_4 X_m Y_n X_m'' Y_n \, dxdy$$

$$m_{42} = \int_0^a \int_0^b - I_4 X_m Y_n X_m Y_n'' \, dxdy \quad , \quad m_{41} = m_{34}$$

$$m_{44} = \int_0^a \int_0^b - I_1 X_m Y_n X_m Y_n \, dxdy + \int_0^a \int_0^b I_6 X_m Y_n X_m Y_n'' \, dxdy + \int_0^a \int_0^b I_6 X_m Y_n X_m'' Y_n \, dxdy$$

The transverse load ***q*** is also given as follows

$$q(x, y) = Q_{mn} \int_0^a \int_0^b \sin(\lambda x) \sin(\mu y) \sin(\lambda x) \sin(\mu y) \, dxdy \tag{20}$$

Table 1 The admissible functions $X_m(x)$ and $Y_n(y)$

	Boundary conditions		The functions $X_m(x)$ and $Y_n(y)$	
	At *x=0, a*	At *y=0, b*	$X_m(x)$	$Y_n(y)$
SSSS	$X_m(0)=X_m''(0)=0$ $X_m(a)=X_m''(a)=0$	$Y_n(0)=Y_n''(0)=0$ $Y_n(b)=Y_n''(b)=0$	$\sin(\lambda x)$	$\sin(\mu y)$
CSCS	$X_m(0)=X_m'(0)=0$ $X_m(a)=X_m''(a)=0$	$Y_n(0)=Y_n'(0)=0$ $Y_n(b)=Y_n''(b)=0$	$\sin(\lambda x)[\cos(\lambda x)-1]$	$\sin(\mu y)[\cos(\mu y)-1]$
CCSS	$X_m(0)=X_m'(0)=0$ $X_m(a)=X_m'(a)=0$	$Y_n(0)=Y_n''(0)=0$ $Y_n(b)=Y_n''(b)=0$	$\sin^2(\lambda x)$	$\sin(\mu y)$
CCCC	$X_m(0)=X_m'(0)=0$ $X_m(a)=X_m'(a)=0$	$Y_n(0)=Y_n'(0)=0$ $Y_n(b)=Y_n'(b)=0$	$\sin^2(\lambda x)$	$\sin^2(\mu y)$

$(\,)'$ denotes the derivative with respect to the corresponding coordinates

4. Numerical results and discussion

In this study, various numerical examples are described and discussed for verifying the accuracy of the present's models in predicting the bending and free vibration behaviors of an antisymmetric cross-ply laminates under different boundary conditions. For the verification purpose, the results obtained by present's models are compared with those of Reddy (1984) and exact solution of three-dimensional elasticity (1970). In order to investigate the efficiency of the present theory, a simpler version of proposed theory (present model) is also developed by omitting the extension component of transverse displacement. The following lamina properties are used:

Material 1[24]: $E_1=40E_2$, $G_{12}=G_{13}=0.6E_2$, $G_{23}=0.5E_2$, $\nu_{12}=0.25$

Material 2[25]: $E_1=40E_2$, $G_{12}=G_{13}=0.5E_2$, $G_{23}=0.6E_2$, $\nu_{12}=0.25$

Material 3[23]: $E_1=25E_2$, $G_{12}=G_{13}=0.5E_2$, $G_{23}=0.2E_2$, $\nu_{12}=0.25$

For convenience, the following non dimensionalizations are used in presenting the numerical results in graphical and tabular forms

$$\bar{w}=\frac{100h^3E_2}{q_0a^4}w(a/2,b/2),\quad \bar{\sigma}_x=\frac{h^2}{q_0a^2}\sigma_x(a/2,b/2),\quad \bar{\sigma}_y=\frac{h^2}{q_0a^2}\sigma_y(a/2,b/2),$$
$$\bar{\tau}_{xy}=\frac{h^2}{q_0a^2}\tau_{xy}(0,0),\quad \bar{\tau}_{xz}=\frac{h}{q_0a}\tau_{xz}(0,b/2),\quad \bar{\omega}=\omega\frac{a^2}{h}\sqrt{\frac{\rho}{E_2}} \tag{21}$$

4.1 Numerical results for bending analysis

The static bending solution obtained by setting the time derivative terms and in-plane forces to zero and simplified as

$$\begin{bmatrix} a_{11} & a_{12} & a_{13} & a_{14} \\ a_{12} & a_{22} & a_{23} & a_{24} \\ a_{13} & a_{23} & a_{33} & a_{34} \\ a_{14} & a_{24} & a_{34} & a_{44} \end{bmatrix}\begin{Bmatrix} U_{mn} \\ V_{mn} \\ W_{bmn} \\ W_{smn} \end{Bmatrix}=\begin{Bmatrix} 0 \\ 0 \\ q \\ q \end{Bmatrix} \tag{22}$$

Table 2 Dimensionless deflections and stresses in two-layer (0°/90°) simply supported (SSSS) square laminated plate under sinusoidal transverse load

a/h	Theory	$\overline{w}$	$\overline{\sigma}_x$	$\overline{\sigma}_y$	$\overline{\tau}_{xy}$
2	Model- Elasticity (Pagano, 1970)	4.9362	-0.9070	1.4480	-0.0964
	Model- Reddy (1984)	4.5619	-1.4277	1.4277	-0.0719
	Present model	4.5728	-1.4256	1.4256	-0.0719
5	Model- Elasticity (Pagano, 1970)	1.7287	-0.7723	0.8036	-0.0586
	Model- Reddy (1984)	1.6670	-0.8385	0.8385	-0.0558
	Present model	1.6680	-0.8380	0.8380	-0.0558
10	Model- Elasticity (Pagano, 1970)	1.2318	-0.7317	0.7353	-0.0540
	Model- Reddy (1984)	1.2161	-0.7468	0.7468	-0.0533
	Present model	1.2164	-0.7467	0.7467	-0.0533
20	Model- Elasticity (Pagano, 1970)	1.1060	-0.7200	0.7206	-0.0529
	Model- Reddy (1984)	1.1018	-0.7235	0.7235	-0.0527
	Present model	1.1019	-0.7235	0.7235	-0.0527
100	Model- Elasticity (Pagano, 1970)	1.0742	-0.7219	0.7219	-0.0529
	Model- Reddy (1984)	1.0651	-0.7161	0.7161	-0.0525
	Present model	1.0651	-0.7161	0.7161	-0.0525

Table 3 The modulus ratio effect on the variation of dimensionless deflection $\overline{w}$ of an antisymmetric cross-ply $(0/90)_4$ square laminates for different boundary conditions

Boundary conditions	a/h	E_1/E_2					
		5	10	20	30	40	50
SSSS	5	2.1533	1.6274	1.2342	1.0708	0.9801	0.9217
	10	1.6332	1.1075	0.7168	0.5567	0.4695	0.4146
	20	1.5025	0.9764	0.5856	0.4257	0.3386	0.2839
	50	1.4659	0.9397	0.5488	0.3888	0.3017	0.2470
	100	1.4606	0.9344	0.5435	0.3835	0.2965	0.2417
CSCS	5	0.5372	0.4350	0.3618	0.3307	0.3125	0.2997
	10	0.3308	0.2298	0.1599	0.1323	.1174	0.1081
	20	0.2786	0.1776	0.1078	0.0804	0.0657	0.0566
	50	0.2640	0.1629	0.0930	0.0656	0.0510	0.0419
	100	0.2619	0.1608	0.0909	0.0635	0.0489	0.0398
CCSS	5	1.5298	1.2258	1.0181	0.9314	0.8804	0.8447
	10	0.9400	0.6401	4425	0.3666	0.3262	0.3009
	20	0.7909	0.4908	0.2936	0.2183	0.1786	0.1540
	50	0.7490	0.4488	0.2515	0.1763	0.1365	0.1120
	100	0.7430	0.4427	0.2455	0.1702	0.1305	0.1060
CCCC	5	1.5210	1.2633	1.0839	1.0041	0.9536	0.9159
	10	0.8375	0.5875	0.4260	0.3642	0.3311	0.3102
	20	0.6637	0.4138	0.2531	0.1925	0.1606	0.1409
	50	0.6149	0.3649	0.2041	0.1435	0.1117	0.0920
	100	0.6079	0.3578	0.1971	0.1365	0.1046	0.0850

A simply supported two-layer (0°/90°) antisymmetric square laminate under sinusoidal transverse load is considered. The layers have equal thickness and Material set 3 is used. Numerical values of dimensionless transverse displacement and inplane stresses are shown in Table 2. Three-dimensional elasticity results are obtained using the method given by Pagano (1970). The results clearly indicate that the percentage error with respect to three-dimensional elasticity solution in predicting the transverse displacement and in-plane stresses is very much lesser in the case of present model and the prediction of in-plane normal stresses $\overline{\sigma}_x$, $\overline{\sigma}_y$ is very poor.

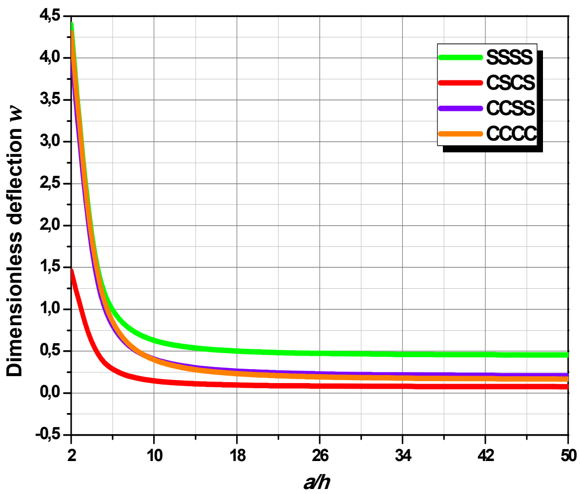

Fig. 2 The effect of side-to-thickness ratio on dimensionless deflection of antisymmetric four-layer (0°/90°)$_4$ square laminates under sinusoidal transverse load for different boundary conditions

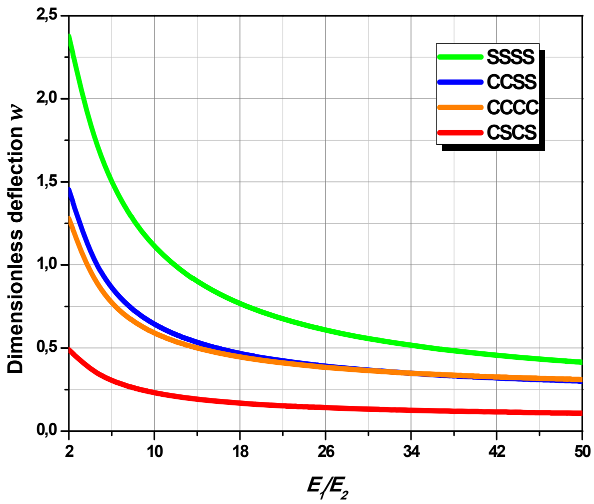

Fig. 3 The effect of modulus ratio on dimensionless deflection of antisymmetric four-layer (0°/90°)$_4$ square laminates under sinusoidal transverse load for different boundary conditions (a/h=10)

Table 4 The aspect ratio effect on the variation of dimensionless deflection $\overline{w}$ of an antisymmetric cross-ply $(0/90)_n$ laminates for different boundary conditions

Number of layers	a/b	Boundary condition			
		SSSS	CSCS	CCSS	CCCC
(0/90)$_1$	0.5	2.4646	0.4643	0.8784	1.1088
	1	1.2161	0.2427	0.6733	0.6032
	2	0.1987	0.0464	0.2213	0.1260
	3	0.0596	0.0162	0.0757	0.0464
	5	0.0148	0.0045	0.0194	0.0130
(0/90)$_2$	0.5	1.2953	0.2790	0.5759	0.7290
	1	0.6865	0.1558	0.4312	0.4189
	2	0.1344	0.0384	0.1558	0.1139
	3	0.0486	0.0157	0.0623	0.0479
	5	0.0146	0.0049	0.0193	0.0145

Table 4 Continued

Number of layers	a/b	Boundary condition			
		SSSS	CSCS	CCSS	CCCC
$(0/90)_3$	0.5	1.1967	0.2613	0.5434	0.6879
	1	0.6382	0.1466	0.4060	0.3969
	2	0.1271	0.0368	0.1478	0.1096
	3	0.0465	0.0151	0.0596	0.0462
	5	0.0141	0.0047	0.0186	0.0139
$(0/90)_4$	0.5	1.1657	0.2555	0.5326	0.6743
	1	0.6229	0.1436	0.3977	0.3895
	2	0.1247	0.0362	0.1451	0.1079
	3	0.0458	0.0149	0.0587	0.0454
	5	0.0139	0.0046	0.0183	0.0135
$(0/90)_8$	0.5	1.1372	0.2502	0.5224	0.6614
	1	0.6087	0.1408	0.3899	0.3825
	2	0.1224	0.0356	0.1425	0.1062
	3	0.0450	0.0146	0.0577	0.0446
	5	0.0137	0.0045	0.0180	0.0132
$(0/90)_{16}$	0.5	1.1303	0.2489	0.5199	0.6582
	1	0.6053	0.1402	0.3880	0.3807
	2	0.1218	0.0355	0.1419	0.1058
	3	0.0449	0.0146	0.0575	0.0444
	5	0.0136	0.0045	0.0179	0.0131
$(0/90)_{32}$	0.5	1.1683	0.2544	0.5292	0.6687
	1	0.6046	0.1400	0.3934	0.3801
	2	0.1198	0.0352	0.1406	0.1054
	3	0.0445	0.0146	0.0571	0.0444
	5	0.0136	0.0045	0.0179	0.0131

The logic of the conditions has been met, where we confirm this logic by presenting the results obtained (Tables 3 and 4) by this method model on the variation of dimensionless deflection of an antisymmetric cross-ply laminates square for different boundary conditions.

To further illustrate the accuracy of present theory for wide range of thickness ratio a/h, material anisotropy E1/E2 and aspect ratio, the variations of dimensionless deflection with respect to thickness ratio, material anisotropy and aspect ratio are illustrated in Figs. 2, 3 and 4, respectively. Again, the present models and existing FSDT give almost identical solutions, whereas CPT underestimates deflections of thick laminates with a/h<20 due to ignoring shear deformation effects (Table 2). The through thickness variations and corresponding values of the in-plane displacement, normal stresses ($\bar{\sigma}_x$, $\bar{\sigma}_y$), and shear stresses ($\bar{\sigma}_{xy}$, $\bar{\sigma}_{xz}$) are also given in Figs. 5,6,7 and 8, respectively, for a moderately thick laminate with a/h=5.

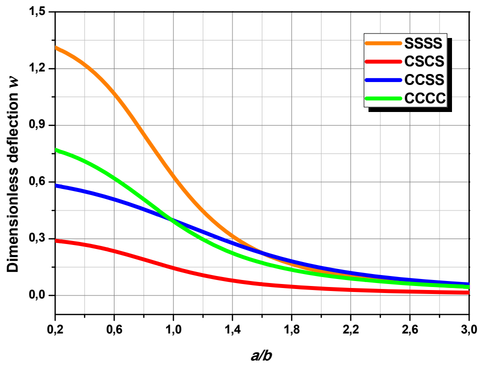

Fig. 4 The effect of aspect ratio on dimensionless deflection of antisymmetric four-layer $(0°/90°)_4$ square laminates under sinusoidal transverse load for different boundary conditions

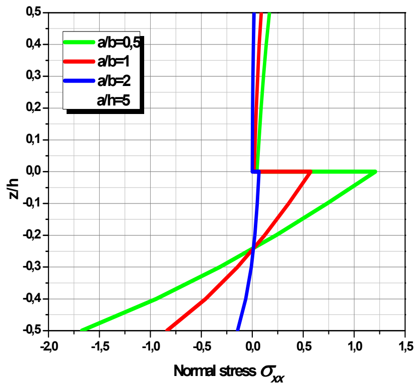

Fig. 5 Variation of normal stress $\bar{\sigma}_x$ through the thickness of simply supported (SSSS) two-layer (0°/90°) square plate for different values of the aspect ratio

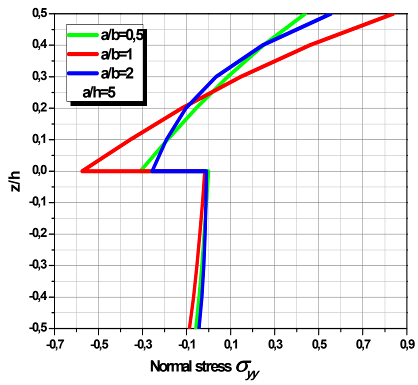

Fig. 6 Variation of normal stress $\bar{\sigma}_y$ through the thickness of simply supported (SSSS) antisymmetric two-layer (0°/90°) square plate for different values of the aspect ratio

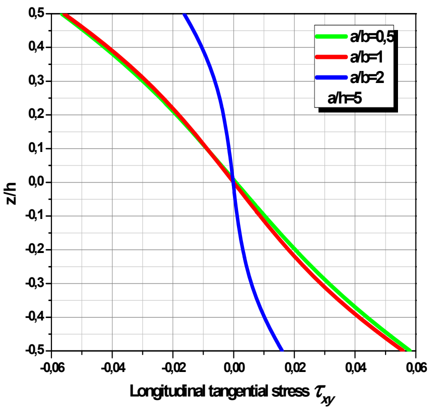

Fig. 7 Variation of longitudinal tangential stress $\bar{\tau}_{xy}$ through the thickness of simply supported (SSSS) two-layer (0°/90°) square plate for different values of the aspect ratio

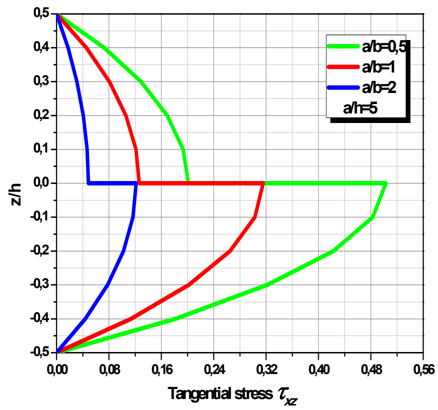

Fig. 8 Variation of tangential stress $\bar{\tau}_{xz}$ through the thickness of simply supported (SSSS) two-layer (0°/90°) square plate for different values of the aspect ratio

4.2 Numerical results for dynamic analysis

In the case of free vibration, the natural frequencies of the laminates can be obtained by setting to zero the determinant of the coefficient matrix of Eq. (23)

$$\left(\begin{bmatrix} a_{11} & a_{12} & a_{13} & a_{14} \\ a_{12} & a_{22} & a_{23} & a_{24} \\ a_{13} & a_{23} & a_{33} & a_{34} \\ a_{14} & a_{24} & a_{34} & a_{44} \end{bmatrix} - \omega^2 \begin{bmatrix} m_{11} & 0 & m_{13} & m_{14} \\ 0 & m_{22} & m_{23} & m_{24} \\ m_{31} & m_{32} & m_{33} & m_{34} \\ m_{41} & m_{42} & m_{34} & ms_{44} \end{bmatrix}\right) \begin{Bmatrix} U_{mn} \\ V_{mn} \\ W_{bmn} \\ W_{smn} \end{Bmatrix} = \begin{Bmatrix} 0 \\ 0 \\ 0 \\ 0 \end{Bmatrix} \tag{23}$$

In Tables 5 and 6, the nondimensional fundamental frequencies of antisymmetrically laminated cross-ply plates obtained by using different shear deformation theories are shown for various values

Table 5 Nondimensional fundamental frequencies of antisymmetric (SSSS) square plates for various values of orthotropy ratio with a/h=5

Lamination	Theory	E_1/E_2				
		3	10	20	30	40
$(0°/90°)_1$	Model- Exact (Noor, 1973)	6.2578	6.9845	7.6745	8.1763	8.5625
	Present Model	6.2168	6.9881	7.8198	8.5028	9.0841
	Model- Reddy (1986)	6.2169	6.9887	7.8210	8.5050	9.0871
$(0°/90°)_2$	Model- Exact (Noor, 1973)	6.5455	8.1445	9.4055	10.1650	10.6790
	Present Model	6.5009	8.1958	9.6273	10.5359	11.1728
	Model- Reddy (1986)	6.5008	8.1954	9.6265	10.5348	11.1716
$(0°/90°)_3$	Model- Exact (Noor, 1973)	6.6100	8.4143	9.8398	10.6950	11.2720
	Present Model	6.5558	8.4053	9.9182	10.8546	11.5009
	Model- Reddy (1986)	6.5558	8.4052	9.9181	10.8547	11.5012
$(0°/90°)_5$	Model- Exact (Noor, 1973)	6.6458	8.5625	10.0843	11.0027	11.6245
	Present Model	6.5842	8.5126	10.0671	11.0191	11.6721
	Model- Reddy (1986)	6.5842	8.5126	10.0674	11.0197	11.6730

Table 6 Nondimensional fundamental frequencies of antisymmetric (SSSS) square plates for various values of a/h with E_1/E_2=40

Lamination	Theory	a/h					
		2	4	10	20	50	100
$(0°/90°)_1$	Present Model	5.7100	8.3507	10.5669	11.1048	11.2750	11.3001
	Model- Reddy (1986)	5.7170	8.3546	10.5680	11.1052	11.2751	11.3002
$(0°/90°)_2$	Present Model	5.7528	9.7366	14.8474	16.5737	17.1850	17.2784
	Model- Reddy (1986)	5.7546	9.7357	14.8463	16.5733	17.1849	17.2784
$(0°/90°)_3$	Present Model	5.8702	9.9870	15.4635	17.3774	18.0644	18.1699
	Model- Reddy (1986)	5.8741	9.9878	15.4632	17.3772	18.0644	18.1698
$(0°/90°)_5$	Present Model	5.9476	10.1226	15.7700	17.7743	18.4984	18.6097
	Model- Reddy (1986)	5.9524	10.1241	15.7700	17.7743	18.4984	18.6097

of a/h and Young's modulus ratios. We can see that, in general, this model gives similar results as the Reddy (1986) and the three-dimensional elasticity solution given in (Noor 1973), in order to predict the natural frequencies.. It should be noted that unknown functions in present model are four; while the unknown functions in the higher-order shear deformation theories (Reddy 1986) is five. It can be concluded that the present model is not only accurate, but also simple in predicting the natural frequencies of laminated plates.

Can be seen in Table 7 that the dimensionless frequencies predicted by this model on the variation of dimensionless deflection of an antisymmetric cross-ply laminates square for different boundary conditions.

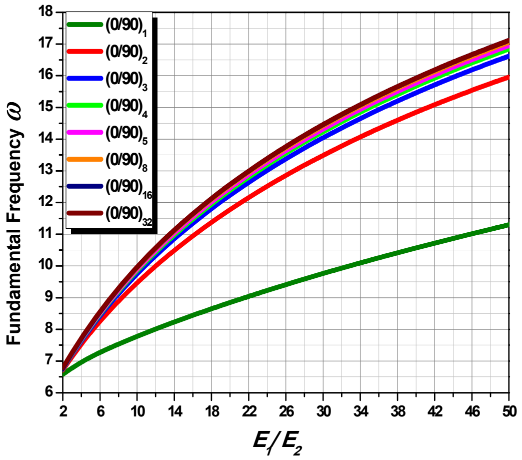

Fig. 9 Variation of dimensionless fundamental frequency of antisymmetric cross- ply $(0/90)_n$ square laminates versus degree of orthotropic (SSSS)

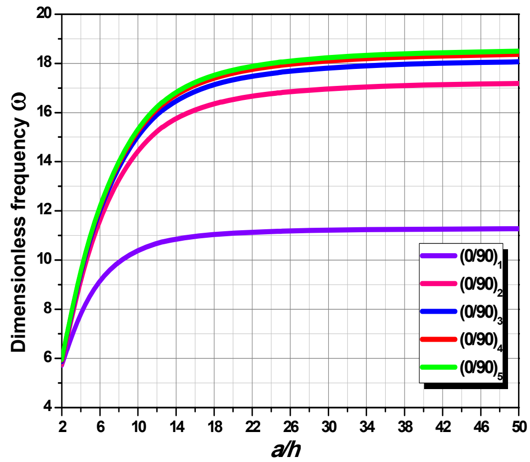

Fig. 10 Variation of dimensionless fundamental frequency of antisymmetric cross-ply $(0/90)_n$ square laminates versus thickness ratio (SSSS)

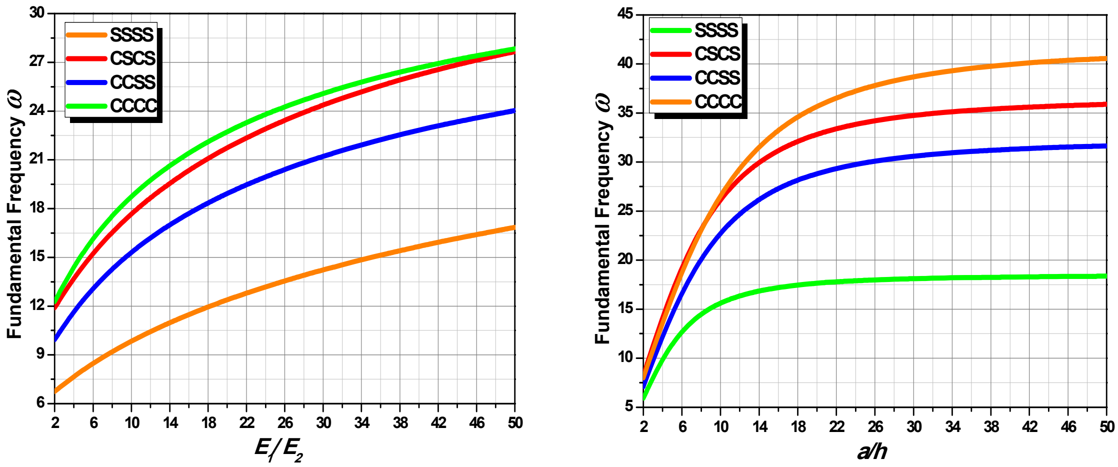

(a) (b)

Fig. 11 Variation of dimensionless fundamental frequency of antisymmetric cross- ply $(0/90)_4$ square laminates for different boundary conditions: (a) degree of orthotropie, (b) thickness ratio

Table 7 Dimensionless fundamental Frequencies $\overline{\omega}$ of antisymmetric cross-ply square plates for different boundary conditions

N° of layers	a/h	Boundary conditions			
		SSSS	CSCS	CCSS	CCCC
$(0°/90°)_1$	5	9.0871	14.9166	12.9658	15.1351
	10	10.5680	19.1522	16.7080	20.5334
	20	11.1052	21.1120	18.4273	23.3691
	50	11.2751	21.8054	19.0320	24.4398
	100	11.3002	21.9114	19.1242	24.6070
$(0°/90°)_2$	5	11.1716	16.4812	14.2097	15.8826
	10	14.8463	25.0846	21.8298	25.6243
	20	16.5733	30.9551	27.1671	33.7361
	50	17.1849	33.5615	29.5762	37.9431
	100	17.2784	33.9935	29.9779	38.6877
$(0°/90°)_3$	5	11.5012	16.8603	14.5312	16.2173
	10	15.4632	25.9454	22.5695	26.3983
	20	17.3772	32.3675	28.4105	35.1953
	50	18.0644	35.2912	31.1191	39.9079
	100	18.1698	35.7805	31.5756	40.7546
$(0°/90°)_4$	5	11.6184	17.0059	14.6557	16.3537
	10	15.6735	26.2441	22.8265	26.6721
	20	17.6496	32.8466	28.8321	35.6913
	50	18.3622	35.8764	31.6408	40.5723
	100	18.4717	36.3852	32.1160	41.4534
$(0°/90°)_5$	5	11.6730	17.0758	14.7156	16.4204
	10	15.7700	26.3821	22.9454	26.7996
	20	17.7743	33.0661	29.0252	35.9187
	50	18.4984	36.1440	31.8794	40.8761
	100	18.6097	36.6616	32.3630	41.7728
$(0°/90°)_8$	5	11.7326	17.1532	14.7821	16.4951
	10	15.8741	26.5316	23.0742	26.9384
	20	17.9084	33.3023	29.2330	36.1636
	50	18.6448	36.4317	32.1359	41.2026
	100	18.7581	36.9588	32.6285	42.1161
$(0°/90°)_{16}$	5	11.7614	17.1910	14.8146	16.5320
	10	15.9239	26.6035	23.1362	27.0053
	20	17.9725	33.4152	29.3324	36.2808
	50	18.7148	36.5693	32.2584	41.3587
	100	18.8291	37.1008	32.7553	42.2802
$(0°/90°)_{32}$	5	11.7693	17.2048	14.8006	16.5441
	10	15.9277	26.6177	22.9629	27.0237
	20	17.9719	33.4193	28.9131	36.2897
	50	18.7122	36.5653	31.6775	41.3554
	100	18.8261	37.0952	32.1439	42.2742

Finally, Figs. 9, 10 and 11 show the variation of dimensionless fundamental frequency of antisymmetric cross- ply $(0/90)_n$ square laminates versus degree of orthotropic and thickness ratio for different boundary conditions.

5. Conclusions

A refined higher-order shear deformation theory of plates has been successfully developed for the static, buckling and free vibration of simply supported laminated plates. The theory allows for a square-law variation in the transverse shear strains across the plate thickness and satisfies the zero-traction boundary conditions on the top and bottom surfaces of the plate without using shear correction factors. The equations of motion were derived from Hamilton's principle. The accuracy and efficiency of the present's models have been demonstrated for static and free vibration behaviors of anti-symmetric cross-ply and angle-ply laminates. The conclusions of this theory are as follows:

- The deflection load obtained using present's models (a simpler version of present theory with four unknowns) and other higher-order theories found in the literature (five unknowns) are almost identical.
- Compared to the three-dimensional elasticity solution, the present's models give more accurate results of static and dynamic load than other higher order shear deformation theory.
- Compared to the three-dimensional elasticity solution, the present's theories give more accurate results of deflection and dynamic load than other higher order shear deformation theory found in the literature.
- The natural frequencies obtained by the proposed model with four unknowns are almost identical to those predicted by the shear deformation theories containing five unknowns.

It can be concluded that the proposed present's models are accurate in solving the static and dynamic behaviors of anti-symmetric cross-ply and angle-ply laminated composite plates and efficient in predicting the vibration responses of composite plates. In perspective we aim a numerical study using the finite element analysis of composite plates Carrera (2002) and Carrera *et al*. (2012).

Acknowledgments

The authors thank the referees for their valuable comments.

References

Abdelhak, Z., L. Hadji, Hassaine Daouadji T. and Adda bedia E.A. (2015), "Thermal buckling of functionally graded plates using a n-order four variable refined theory", *Adv. Mater. Res.*, **4**(1), 31-44.

Ait Amar Meziane, M., Abdelaziz, H.H. and Tounsi, A. (2014), "An efficient and simple refined theory for buckling and free vibration of exponentially graded sandwich plates under various boundary conditions", *J. Sandwich Struct. Mater.*, **16**(3), 293-318.

Aydogdu, M. (2009), "A new shear deformation theory for laminated composite plates", *Compos. Struct.*, **89**(1), 94-101.

Benferhat, R., Hassaine Daouadji, T. and M. Said Mansour (2014), "A higher order shear deformation model for bending analysis of functionally graded plates", *Transactions of the Indian Institute of Metals*, **68**(1), 7-16.

Bouazza, M., K. Amara, M. Zidour, A. Tounsi and El A. Adda Bedia (2015), "Postbuckling analysis of functionally graded beams using hyperbolic shear deformation theory", *Rev. Inform. Eng. Appl.*, **2**(1), 1-14.

Bouazza, M., K. Amara, M. Zidour, A. Tounsi and El A. Adda Bedia (2015), "Postbuckling analysis of nanobeams using trigonometric Shear deformation theory", *Appl. Sci. Reports*, **10**(2), 112-121.
Carrera, E. (2002), "Theories and finite elements for multilayered, anisotropic, composite plates and shells", *Archiv. Comput. Meth. Eng.*, **9**(2), 87-140.
Carrera, E. and Miglioretti, F. (2012), "Selection of appropriate multilayered plate theories by using a genetic like algorithm", *Compos. Struct.*, **94**(3), 1175-1186
Hassaine Daouadji, T., Tounsi, A. and Adda bedia, E.A. (2013), "Analytical solution for bending analysis of functionally graded plates", *Scientia Iranica, Trans. B: Mech. Eng.*, **20**(3), 516-523.
Hebali, H., A. Tounsi, S. Houari, A. Bessaim and E.A. Adda Bedia (2014), "A new quasi-3D hyperbolic shear deformation theory for the static and free vibration analysis of functionally graded plates", *J. Eng. Mech.*, ASCE, **140**(2), 374-383.
Karama, M., K.S. Afaq, and S. Mistou (2003), "Mechanical behavior of laminated composite beam by the new multi-layered laminated composite structures model with transverse shear stress continuity", *Int. J. Solid. Struct.*, **40**(6), 15251546.
Karama, M., Afaq, K.S. and Mistou, S. (2009), "A new theory for laminated composite plates", *Proceeding of the IMechE, vol. 223* (Part L: Journal of Materials: Design and Applications).
Mahi, A., E. Adda Bedia and A. Tounsi (2015), "A new hyperbolic shear deformation theory for bending and free vibration analysis of isotropic, functionally graded, sandwich and laminated composite plate", *Appl. Math. Model., Appl. Math. Model.*, **39**(9), 2489-2508.
Mantari, J.L., A.S. Oktem and C. Guedes Soares (2012), "A new trigonometric shear deformation theory for isotropic, laminated composite and sandwich plates", *Int. J. Solid. Struct.*, **49**(1), 43-53.
Meiche, N.E., Tounsi, A., Ziane, N., Mechab, I. and Bedia, E.A. (2011), "A new hyperbolic shear deformation theory for buckling and vibration of functionally graded sandwich plate", *Int. J. Mech. Sci*., **53**(4), 237-247.
Mindlin, R.D. (1951), "Influence of rotary inertia and shear on flexural motions of isotropic, elastic plates", *J. Appl. Mech.*, **18**, 31-38.
Nedri, K., N. El Meiche and A. Tounsi (2014), "Free vibration analysis of laminated composite plates resting on elastic foundation by using a refined hyperbolic shear deformation theory", *Mech. Compos. Mater.*, **49**(6), 629-640.
Noor, A.K. (1975), "Stability of multilayered composite plate", *Fibre Sci. Technol.*, **8**(2), 81-89.
Noor, K. (1973), "Free vibrations of multilayered composite plates", *AIAA J.*, **11**(7), 1038-1039.
Pagano, N.J. (1970), "Exact solutions for rectangular bidirectional composites and sandwich plates", *J. Compos. Mater*., **4**(1), 20-34.
Reddy, J.N. (1984), "A simple higher-order theory for laminated composite plates", *J. Appl. Mech*., ASME, **51**(4), 745-752.
Reddy, J.N. (1986), "A refined shear deformation theory for the analysis of laminated plates", *NASA Report 3955*.
Reissner, E. (1945), "The effect of transverse shear deformation on the bending of elastic plates", *J. Appl. Mech., Trans*., ASME, **12**(2), 69-77.
Ren, J.G. (1986), "A new theory of laminated plate", *Compos. Sci. Technol*., **26**(3), 225-239.
Ren, J.G. (1990), "Bending, vibration and buckling of laminated plates", Ed., Cheremisinoff, N.P., Handbook of ceramics and composites, **1**, 413-450.
Shimpi, R.P. and Patel, H.G. (2006), "A two variable refined plate theory for orthotropic plate analysis", *Int. J. Solid. Struct.*, **43**(22), 6783-6799.
Shimpi, R.P. and Patel, H.G. (2006), "Free vibrations of plate using two variable refined plate theory", *J. Sound Vib*., **296**(4-5), 979-999.
Tlidji, Y., Hassaine Daouadji, T., Hadji, L., Tounsi, A. and Adda bedia, E.A. (2014), "Elasticity solution for bending response of functionally graded sandwich plates under thermo mechanical loading", *J. Therm. Stress*, **37**(7), 852-869.
Tounsi, A., Sid Ahmed, H., Benyoucef, S. and Adda Bedia, E.A. (2013), "A refined trigonometric shear deformation theory for thermoelastic bending of functionally graded sandwich plates", *Aero. Sci. Technol.*, **24**(1), 209-220.

Zenkour, A.M. (2006), “Generalized shear deformation theory for bending analysis of functionally graded plates”, *Appl. Math. Model.*, **30**(1), 67-84.

CC